Deep Constitutional Neural Networks based on VGG-16 Transfer Learning for Abnormalities Peeled Shrimp Classification

Tamnuwat Valeeprakhon[1], Korawit Orkphol[2], and Penpun Chaihuadjaroen[3]

[1,2,3]Department of Computer Engineering, Faculty of Engineering at Sriracha,
Kasetsart University Sriracha Campus.
E-mail: tamnuwat@eng.src.ku.ac.th, korawit@eng.src.ku.ac.th, penpun@eng.src.ku.ac.th

Received: September 27, 2021 / Revised: October 29, 2021 / Accepted: November 10, 2021

***Abstract*—Peeled white leg shrimp is an important exports economic product of many countries within the coastal areas. In the shrimp processing, shrimps are beheaded and peeled with an automatic machine; after that, the peeled shrimps will be inspected to classify the well-peeled shrimps from the abnormal peeled shrimps. However, the inspection process is conducted in manual work, and this may result in misinterpretation and reduce the manufacturing efficiency due to exhausted humans. Nowadays, machine learning plays an important role in food industries for monitoring manufacturing quality activities. This powerful technology has made significant breakthroughs in this field and their performances greatly surpass human work. In this paper, a deep convolutional neural network based on VGG-16 transfer learning for abnormalities in peeled shrimp classification is proposed. This method makes up two of the main steps preprocessing and model network definition. The dataset preprocessing aims to prepare the provided dataset to suit our classification model by aligning images into the C shape pattern, cropping, and resizing images to meet the need of VGG-16 input layer requirement. The network model definition aims to build the classification model by considering the VGG-16 transfer learning model. This model was customized by replacing the old classification layer with our designed fully connected layers and was trained by using the best parameters conducted in the experimental process. The results obtained from our VGG-16 model achieve 98.36% of accuracy with 0.0213 seconds for classification time, and it produces better results than other comparative models.**

***Index Terms*—Abnormalities Peeled Shrimp, VGG-16, Transfer learning, Image classification**

I. Introduction

White leg shrimp or Litopenaeus Vannamei is a type of marine shrimp that is native to South America and commonly found in the coastal regions of the Eastern Pacific Ocean from northern Mexico to northern Peru [1]. Nowadays, white leg shrimp farming is widely popular worldwide because these shrimps have a fast growth rate, good adaptability the various environmental conditions, and high consumer demands. According to a survey of global shrimp exports, shrimp frozen is the world's 137th most traded product, with a moreover total trade of $19 billion [2].

White leg shrimp is an important export economic product of many countries such as India, Ecuador, Vietnam, Thailand, etc. [3]. The exported shrimp must be processed to preserve freshness and high quality. However, preserving the shrimp quality is very difficult because the dead shrimps will be decomposed rapidly through the Self-Autolysis process; the internal organs in the shrimp head release enzymes such as Tyrosine, Tryptophane, and Cystine. These enzymes spread to the other organs, and the external microorganisms enter the shrimps, causing the flesh color of the shrimps to turn opaque white to yellow, indicating the shrimps were degraded quality [4].

Freezing is one of the most popular shrimp processing to preserve the shrimp quality by reducing the temperature of the shrimp to below -18° degrees, the water in the shrimp turns into ice. This process will preserve the freshness and quality better than other food processing techniques [4]. Frozen shrimp is a product that has been processed by freezing processing. It is popular in many countries because it is cheap, easy to cook, and has a variety of health benefits. The exported frozen shrimp consists of frozen whole shrimp, frozen peeled shrimp, frozen

peeled and tail-on shrimp, frozen be-headed shrimp, and frozen boiled shrimp [5].

The frozen peeled shrimp is the most popular frozen exported shrimp the processing of this frozen shrimp consists of several steps: The first step, the shrimps are washed in clear water at a temperature below 0^{o} degrees to reduce the microorganism, the next step, these shrimp are sorted according to their size, then, these shrimps are beheaded to reduce the self-Autolysis of the chemicals in internal organs in the head of shrimp, the next step, the behead shrimps are peeled to reduce microbial contamination, then, the peeled shrimps are inspected for classifying the abnormalities of peeled shrimps and fixing them, and the last step, the peeled shrimp are frozen at a temperature below -18^{o} degrees to preserve the quality of their shrimps [6].

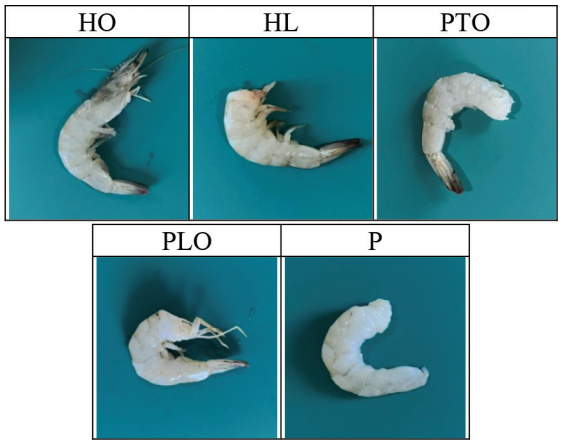

Fig. 1. The Abnormalites of peeled shrimps. Normal peeled shrimp (P) and abnormal peeled shrimp consists of: Whole or Head-on (HO), Headless (HL), Peeled tail-on (PTO), and Peeled leg-on (PLO)

The inspection process detects the abnormalities of peeled shrimps since the shrimps are peeled by a high-speed automatic machine. Sometimes, the employees will detect the abnormalities of peeled shrimps with incomplete problems consisting of four types as follows: whole or head-on (HO) is un-peeled shrimp and their head has not been cut, headless (HL) is un-peeling, but their head has been cut, peeled tail-on (PTO) is peeled shrimp but their tail has remained, and peeled leg-on (PLO) is peeled shrimp, but their leg has not been removed. An example normally (P) and the abnormalities peeled shrimp images are shown in Fig. 1. However, classification and inspection of peeled shrimps are difficult and still depend on manual work, as a consequence of misjudgments and reduce the manufacturing efficiency because exhausted humans.

Nowadays, computer vision technology plays an important role in the food industry, mainly including food safety and quality evaluation [7], food process monitoring and packaging [8], and foreign object detection [9]. This technology has more advantages than human manual work, and this may result in increasing manufacturing efficiency and reliability and releasing humans from labor. Moreover, computer vision is becoming popular in the food industry, especially the shrimp industry. In the past few years, computer vision techniques have been applied to the field of the shrimp industry as follows: Trung Thanh N Thai proposed the a method for estimating shrimp population density and calculating the size of the shrimp based on computer vision techniques [10], R. P. Surya Sanker presented the infected shrimp with the white spot disease classification based KNN machine learning [11], Dah Jye Lee provided the method for evaluating the quality of shrimp based on image processing techniques [12], Dong Zhang proposed the method for grading shape of shrimps by using Evolution-constructed based machine learning [13], and Zihao Liu presented the method for segmenting the touching pairs of cooked shrimp in order to evaluate the quality of their shrimp [14].

The majority of the research focused on shrimp segregation, size monitoring quality control, and disease detection using image processing and machine learning techniques. However, there are no researchers on the peeled shrimp quality inspection. The automated peeled shrimp inspection is very challenging since nobody has done this before and the developed applications should outperform human efficiency. Transfer learning is a class of machine learning techniques and it is very popular in image classification tasks by using the existing knowledge to solve different problems. This powerful technology is used in many real industrial applications and it can classify the quality of a product via appearance images [15]. In order to classify the abnormalities of peeled shrimps, a transfer learning technique will become to solve this problem.

This paper proposed a deep learning method based on VGG-16 [16] transfer learning network architecture to classify the abnormalities of the peeled shrimp which consists of four types: HO, HL, PTO, and PLO. Our proposed method includes two main steps: dataset preprocessing, and definition of a training network composed of a pre-trained model, future extraction, and the abnormalities peeled shrimp classification.

The remainder of this paper is organized as follows: The first part is aimed to introduce a statement of the problem. The second part describes the experimental setup for the white leg shrimp classification with transfer learning. In the third part, the experimental results are presented. The fourth in the art, the experimental analysis is discussed by comparing with other transfer learning and traditional supervised learning methods. Finally, the last part summarizes the paper and, future work is carried out.

II. Methodology

Our proposed approach aims to classify the abnormalities of peeled shrimp images, and it makes up of two main steps: Data preprocessing, and VGG-16 architecture definition. Since the provided dataset was photographed with disordering and the size of image does not meet the need of the VGG-16 input layer requirement. Data preprocessing aims to prepare the provided dataset by aligning all the peeled shrimps in images into the same pattern and resizing these images to match the requirement of the VGG-16. The use of VGG-16 as transfer learning requires a classification layer customization. The VGG-16 architecture definition aims to customize the classification layer by replacing the old one with our fully connected layer architecture. Our proposed approach is presented as the following.

A. Data Preprocessing

The dataset is obtained from the peeled shrimp images that are simulated to cover all forms of the peeled shrimp abnormalities and these images will be grouped according to their class. Each image is taken with the same focal length in the same environment and a resolution of 1,280x960 pixels.

The VGG-16 requires a complex dataset with a specific symmetrical size of image for building a powerful classification model. However, the provided dataset is generated from disordered images, and there are no symmetrical sizes that can directly affect our classification model efficiency. To overcome these problems, aligning and resizing the image will be applied. Image alignment is a process to compute the transformation that aligns the dataset into the same pattern, and image resizing is the process to reduce the dimension of images. However, resizing the large image to a smaller size may result in a loss of quality and missing features of interesting objects in case of these objects are very smaller than the image size. Therefore, the object should be cropped with an asymmetrical size before resizing to maintain the high quality and good features of the objects.

Fig. 2 gives an overview of the data preprocessing procedure consisting of four main steps: (1) The background extraction based on color segmentation, (2) noise and hole removal using morphological operation opening follow by closing, (3) the image alignment based on skeletonization, and (4) object region identification based symmetrical bounding box calculation and cropping region.

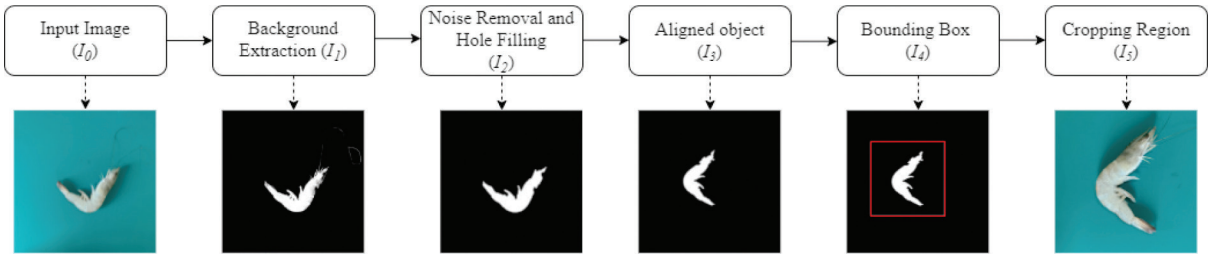

Fig. 2. Overview of the dataset preprocessing method

1)Background Extraction

The segmentation-based color [17] is the powerful method for extracting the interested object from a color image by considering values of the color spaces. It is very important to select the right color space for the right jobs as they will provide a good result on extracting objects. The color spaces selection is determined by the distribution of each value of each color channel, and their value should be clearly differentiated from each others. Fig. 3 shows the distributed values of each color space of a shrimp image, and the result shows that CIELab [18] color space provides a different distribution of each channel value than other candidate color spaces i.e., HSV [19], RGB [20], YCbCr [21].

The CIELab color space is a device-independent color model. This color model is not relative to any particular devices and covers the entire range of human color perception.

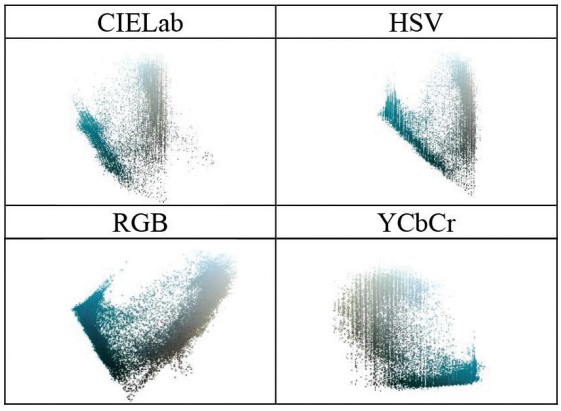

Fig. 3. The distribution values of CIELab, HSV, RGB, and YCbCr color space

Therefore, the CIELab is a useful color model in image processing to segment object jobs where L, A, and B represent Lightness, the position of color between red and green, and the position of color between yellow and blue, respectively. In this research, the CIELab color segmentation can extract the background from a shrimp object by converting input image I_0 from RGB color space into the CIELab color space, then limiting the range of L to 50-100, and B to 0-127. The result of this step is a binary image, as shown in Fig. 2 with I_1.

2) Noise Removal and Hole Filling

Once the background was extracted off from the object, noises and holes are always appear over the segmented binary image. Noise is a small group of white pixels surrounded by a lake of black pixels, while a hole is a group of back pixels surrounded by white pixels of an interested object. The removal of holes and noises can be performed by using image processing techniques with morphological opening followed by closing [22]. The morphological opening operation is powerful for handling small noise by eroding an image and then dilating the eroded images, while the morphological closing operation is great for filling small holes by dilating an image and then eroding the dilated image. The result after using the opening and closing operation is shown in Fig. 4 with I_2.

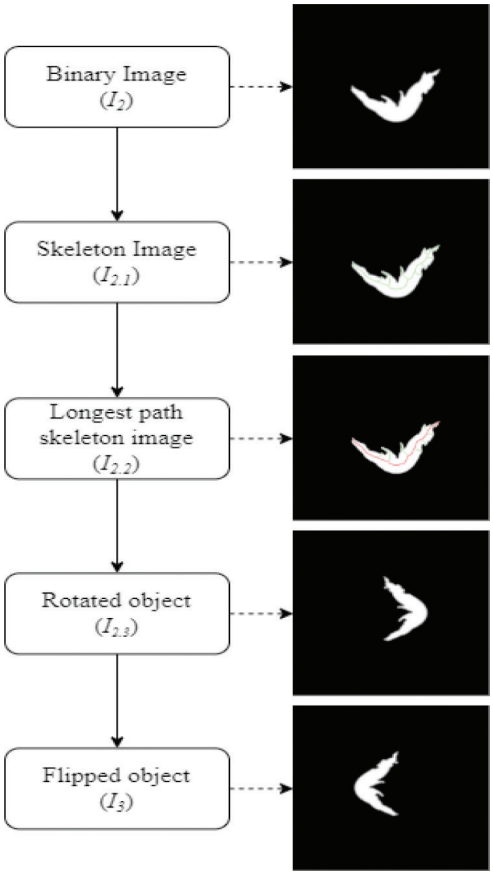

Fig. 4. Overview of object alignment method

3) Object Alignment

The binary image I_2 was presented after noises and holes removing, then the object alignment will be calculated. Fig. 4 shows an overview of an object alignment procedure by considering the characteristic of a skeleton of shrimp that has a shape like the C and these shrimps will be aligned into this pattern.

The skeleton is extracted from I_2 by reducing a white region in a binary image to a skeletal remnant that largely preserves the extent and connectivity of the original region. The skeleton can be expressed in terms of morphological erosions and openings [23] by using formula 1-2 and the skeletonized image is shown in Fig. 4.

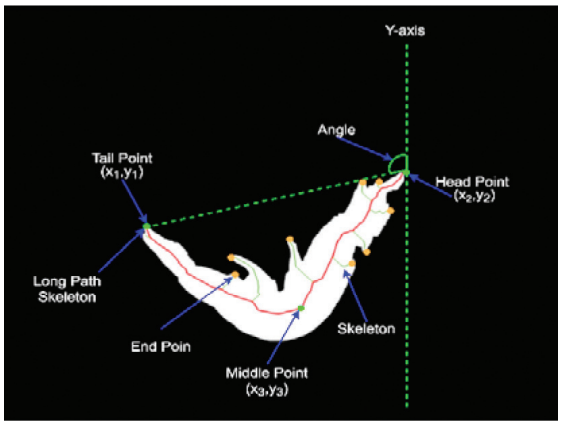

Fig. 5. Skeleton of an object represents in green color, the long path of the skeleton represents the red color and the angle of rotation represents the green angle.

The skeleton is made up of many branches connected to many paths. The C pattern will be identified by observing the longest path of the skeleton as shown in Fig. 5. The longest path is identified by finding every endpoint (The orange and green points) of the skeleton and paring these points in order to find the length between the paired points. The longest path of the skeleton is a path between the endpoint at the head of the shrimp and the endpoint at the tail of the shrimp (The green points) where a path formed by these points provide a maximum length.

$$S(A) = \bigcup_{k=0}^{K} S_k(A) \quad (1)$$

$$S_k(A) = \bigcup_{k=0}^{K} \{(A!\ kB) - [(A!\ kB) \circ B]\} \quad (2)$$

Where B is a structure element, $(A!\ kB)$ indicates k successive erosions of A, and K is the last iterative step before A erodes to an empty set.

$$\theta = \cos^{-1}\left(\frac{Y_1 - Y_2}{\sqrt{(x_1 - x_2)^2 + (Y_1 - Y_2)^2}}\right) \quad (3)$$

Where $Y_1 = \max(y_1, y_2)$ and $Y_2 = \min(y_1, y_2)$

The shrimp will be aligned into the C pattern by rotating this shrimp to the vertical with the Angle of Rotation (AoR). Fig. 5 shows the AoR which is the angle between the Y-axis and the line between the head point and the tail point of the shrimp, this angle is performed with formula 3, and the rotated image is shown in Fig. 4 ($I_{2.3}$). However, the shrimp can be flipped on the left or right hand. If the shrimp was flipped to the right hand, it would be flipped back to the left by observing the middle point of the longest path of the skeleton. The x coordinate of this point would be less than the x coordinate of the head and tail points. The flipped image is shown in Fig. 4 (I_3).

4) Symmetrical Bounding Box Calculation and Cropping Region

The most of the images are used to train the machine learning models are symmetrical size, so the cropped images must also be symmetrical. The Bounding Box (BB) is a popular method for identifying the cropping region that fits the interested object [24] as shows in Fig. 6 with the red rectangle. However, this method is not suitable for this research because the cropped object is asymmetrical. The Symmetrical Bounding Box (SBB) is our modified of Bounding Box (BB) method to calculate the cropping region in order to crop an interested object with a symmetrical size. This method uses a list of boundary points for calculating their cropping region.

The Border Following (BF) is one of the fundamental techniques in the image processing of digitized binary images, it is used to address the boundary of object region by driving a sequence of coordinates or the chain codes from the boundary between white region and background [25]. Once the BF was applying, the result of this method represents a list of the pixel coordinates of region boundary as formula 4, then SBB will be calculated by using the formula 5-6.

$$list_x = [x_1, x_2, x_3 ... x_n] \quad (4)$$
$$list_y = [y_1, y_2, y_3 ... y_n]$$

$$cropping = (start_x, start_y) \text{ to } (end_x, end_y) \quad (5)$$

$$start_i = \frac{\min(list_i)}{2} + \frac{\max(list_i)}{2} - \frac{\partial}{2} - \beta \quad (6)$$
$$end_i = \frac{\min(list_i)}{2} + \frac{\max(list_i)}{2} + \frac{\partial}{2} + \beta$$
$$\partial = \max(\max(list_x) - \min(list_x), \max(list_y) - \min(list_y))$$

Where, $i \subset \{x, y\}$ and β is margin size

Fig. 6 shows a result obtained from SBB with a margin of 100 with the green rectangle. This method provides a starting point and ending point in order to crop a region with a symmetrical rectangle surrounding the interesting object while the BB provides a rectangle that fits the object as the red rectangle. All input images will be cropped with the symmetrical rectangle obtained from SSB, and the cropped images have a space between the object and the border in order to prevent miss featured in the feature extraction process all of the cropped images are resized into 224x244 pixels to serve the requirement of the VGG-16 input layer. Table I shows the example cropped images categorized by class of the abnormities of peeled shrimp.

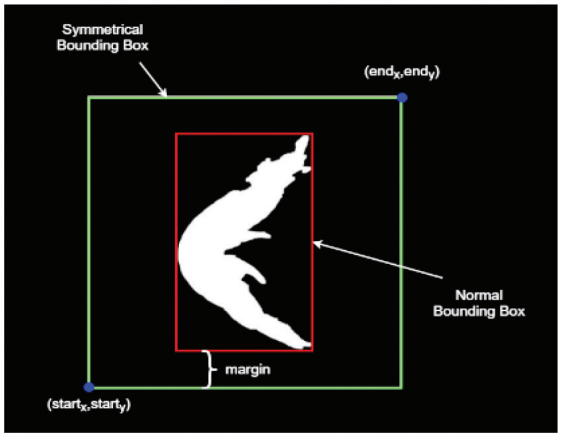

Fig. 6. The green rectangle is a result obtained by SBB and the red rectangle is a result obtained by BB the symmetrical.

B. Dataset and VGG-16 Architecture Definition

Transfer learning is a machine learning method based on a convolutional neural network. This method uses existing knowledge to solve different tasks but related filed of problems. Generally, the machine learning method requires a sufficient dataset and perfect network architecture to build a model for classifying multi-class of problems through the learning process. However, the transfer learning method uses less dataset and learning time than other machine learning methods because it uses a pre-trained weight as the starting point for learning cause the speed up for training and the performance of the classification model has been improved.

1) Dataset

The peeled shrimp dataset consists of a total 5,074 of color images out of which 880 are normal peeled shrimps (P), 1004 are abnormal unpeeled shrimps, and their head still on (HO), 1,272 are abnormal unpeeled shrimps but their heads are beheaded (HL), 950 are abnormal peeled shrimps but their tail still on (PTO), and 968 are abnormal peeled shrimps but their leg still on (PLO). Table I shows the example labeled dataset by classes. All images are pre-processed and normalized resulting in an image size of 224x224 with all pixel values in a range of 0-1 that meet the need of the VGG-16 input layer requirement. This dataset is split randomly into three parts for training, validating, and testing our classification model. The first spitted dataset is used to fit the model and consists of 60% of all datasets and the remaining is equally split for validating and testing (20% for validation and 20% for testing).

TABLE I
THE ABNORMAITIES PEED SHRIMP DATASET

Label	Type	Class	Status	Example	Sample
0	Whole or Head-on	HO	Abnormal		1,004
1	Headless	HL	Abnormal		1,272
2	Peeled Tail-on	PTO	Abnormal		950
3	Peeled Leg-on	PLO	Abnormal		968
4	Peeled	P	Normal		880

2) VGG-16 Architecture

VGG-16 is sixteen layers based on convolutional neural network architecture used by the Visual Geometry Group from Oxford University to obtain outstanding results in the ILSVRC2014(Large Scale Visual Recognition Challenge 2014) competition [16]. It was still considered to be an excellent model in the classification task. This model uses a set of weights pre-trained on ImageNet and it achieves 92.5% which currently in top five test accuracy in ImageNet [26].

Fig. 7 shows the architecture of the VGG-16 network consists of thirteen convolutional layers and three fully connected layers. However, the use of the VGG-16 as a transfer learning will require to freeze all the weight layers from trainable to non-trainable and create a new fully connected layers that fits the new dataset instead of the three old layers on top of the output layers from the base model. The characteristics of VGG-16 used in our work are as follows:

- The input layer uses 224x224x3 pixels of image size.
- The whole convolution layer uses a kernel size of 3x3 with a stride size of 1 and sets the padding as the same. The used pooling layers are max pooling with 2x2 layers with a stride size of 2. VGG 16 uses the Rectified Linear Unit as the activation function with the formula (7).

$$\text{Relu}(x) = \max(0, x) \tag{7}$$

- In the classification task, cross-entropy is used as a loss function to assess the true and predicted value with formula (8) $y(x_i)$ where represents the true label and $\hat{y}$ (xi) represents the prediction label. The loss of each batch is shown in formula (9) where n represents the category number and m is the sample number in the batch.

$$\text{H} = -\sum_{i=1}^{n} y(x_i)\log(\hat{y}(xi)) \tag{8}$$

$$\text{loss} = -\frac{1}{m}\sum_{j=1}^{m}\sum_{i=1}^{n} y = y_{ji}\log(\hat{y}_{ji}) \tag{9}$$

- The output layer uses Softmax as a probability distribution which is the highest probability with the formula (10). In order to classify tasks, there are five categories m in multi-classification prediction. The label Y has m values where $y^{(i)} \in \{0,1...,m\}$ is a category in sample space. $p = (y = j \mid x)$ represents the probability that x belongs to an exact category j=1,2...,m. The classifier parameters represent as $\theta = [\theta_1^t, \theta_2^t, ..., \theta_m^t]$. Thus, the probability will belong to a certain class.

$$h_\theta(x^{(i)}) = \begin{bmatrix} p(y^{(i)} = 0 \mid x^{(i)}; \theta) \\ p(y^{(i)} = 1 \mid x^{(i)}; \theta) \\ \vdots \\ p(y^{(i)} = m \mid x^{(i)}; \theta) \end{bmatrix} = \frac{1}{\sum_{j=1}^{m} e^{\theta_j^t x^{(i)}}} \begin{bmatrix} e^{\theta_1^t x^{(i)}} \\ e^{\theta_2^t x^{(i)}} \\ \vdots \\ e^{\theta_m^t x^{(i)}} \end{bmatrix} \tag{10}$$

The old classification layer with three fully connected was replaced with our designed classification layer that is suited for our task as shown in Fig. 6. Our proposed model-based transfer learning is trained by using the best parameters conducted in the experiment process consisting of the optimization algorithm with Adam, training iterate with 1000 epoch, 128 of batch size and learning rate with 0.001. The overfitting problem will be eliminated by setting the early stopping with 3 of patience which refers to the number of epochs with no improvement after training and it will be stopped.

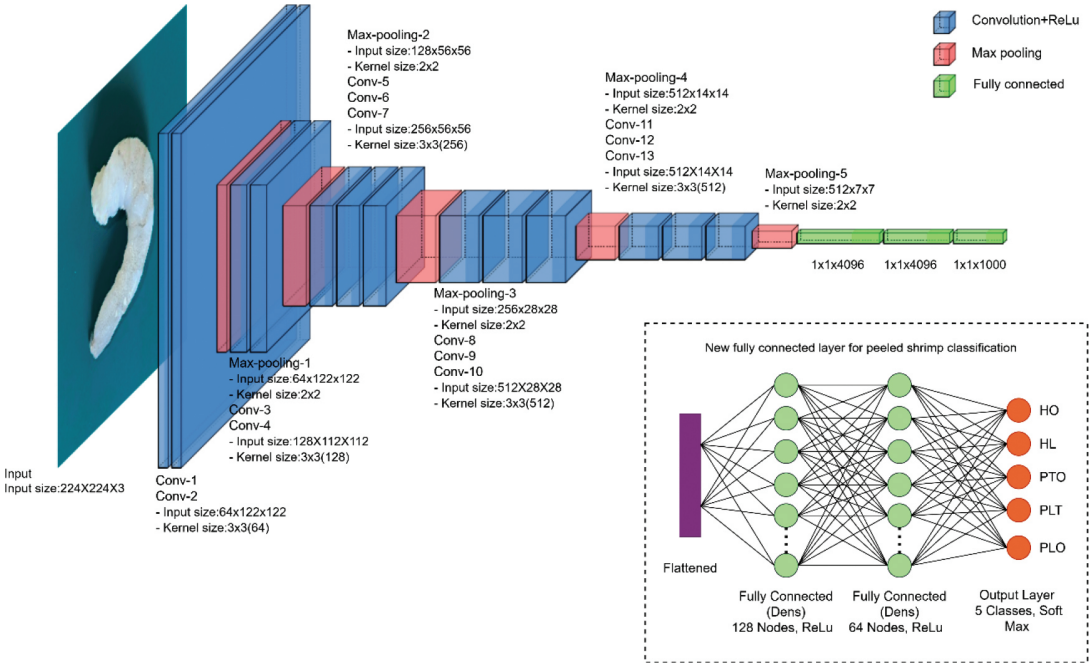

Fig. 7. VGG 16 network architecture by freezing the last three old Fc layers and replaces it with our designed Fc layers.

III. Results And Discussion

The experimental results of our proposed the VGG-16 transfer learning based on the abnormities peeled shrimp classification are statistically described as accurate compared with the difference models including five transfer learning models and three supervised learning models by considering the various confusion matrix-based performance matrices. These metrics consist of four main indicators: (1) Accuracy is characterized as the percentage of relevant results measuring all the correctly classification class. (2) Precision is used to evaluate exactness of a classification model. (3) Recall is the measure of completeness of a classification model. (4) F-measure is defined as the weighted harmonic mean of precision and recall [28].

All experimental methods in this paper were programmed in Python version 3 and there ware implemented on the NVIDIA DGX1 AI cloud server, CPU Dual 20-core Intel Xeon E5-2698 v4 2.2 GHz, GPUs 8X NVIDIA Tesla V100, and 512 GB 2,133 MHz DDR4 of system memory.

In order to evaluate our proposed models, it is necessary to run the training model with several times to determine the average accuracy because the classification model requires random data for training, validation and testing, which may result in an accuracy instability.

Table II represents the results obtained from VGG-16 models running in 35 times, our testing results achieve 98.36% in average of accuracy with 0.0213 seconds on a classification time and the model size is 64.54 MB. All indicators produce good and consistent results, and the standard deviation of all indicators is very small since our proposed method provides the result clustered around the mean.

TABLE II
THE COMPARISON MEAN OF ACCURACY, PRECISION, RECALL, F-MEASURE, PREDICTION TIME AND MODELS SIZE

Method	Model	Accuracy (%)	Precision (%)	Recall (%)	F-measure (%)	Time (Sec)	Size (MB)
Transfer Learning	VGG16	98.36	98.46	98.45	98.42	0.0213	64.54
	MobileNet	97.45	97.54	97.59	97.55	0.0159	19.49
	Xception	94.95	95.24	95.15	95.09	0.0240	91.70
	Resnet-50	97.44	97.54	97.56	97.50	0.0249	102.56
	Densnet	98.06	98.18	98.18	98.13	0.0514	82.25
	Inception	96.18	96.25	96.44	96.28	0.0076	93.37
Supervised Learning	SVM	74.81	75.64	77.33	75.03	0.0091	0.400
	CNN	91.01	91.32	91.46	91.19	0.0093	2.170
	RNN	77.95	78.02	79.65	77.00	0.0004	0.280

Fig. 8(a) represents the training and validating accuracy curves of the VGG-16 model which was trained with a pre-processed dataset. These curves are increasing and flatting closely to 100% of accuracy. Fig. 8(b) represents the training and validation loss curves that the validation loss is slightly greater than the training loss. These curves are decreasing and flat to the point of stability after 100 epochs until the end. This kind of curve represents the best fit learning curve [29]. Fig. 8(c) represents the confusion matrix of the impact of false class rates. This matrix provides the rich of true positives and true negatives accuracy for each class while false positives and false negatives are very small. Therefore, it can be concluded that the VGG-16 model training has a good effect, keeping a few losses, owing to validating the accuracy and avoiding being affected by the over-fitting problem.

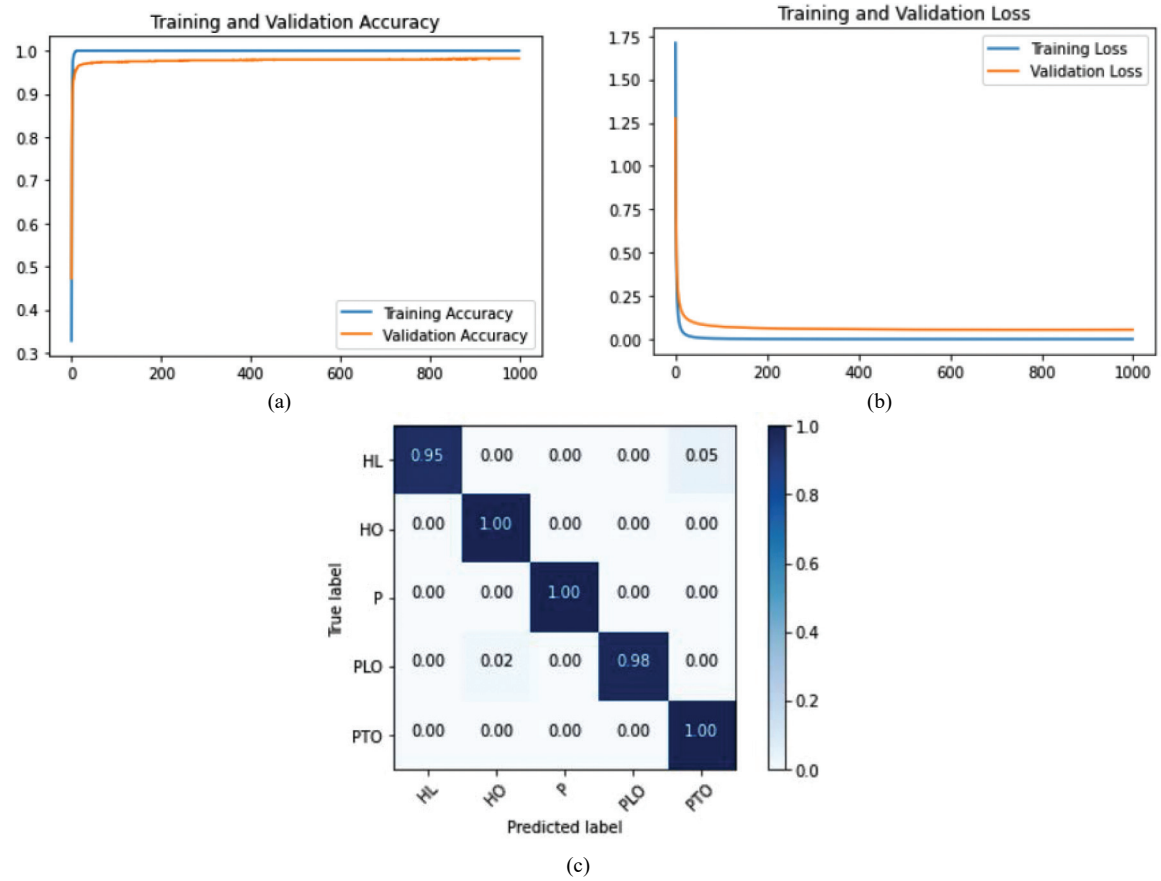

Fig. 8. Training and Validating analysis over 1,000 epochs: (a) Training and validating accuracy analysis, (b) Training and validating loss analysis, (c) Confusion Matrix analyses of VGG-16 trained with preprocessed dataset.

Fig. 9 represents the comparison accuracy between the VGG-16 models that were trained with and without a preprocessed dataset. These models were trained with the same parameter setting and were ran in 35 times with 1000 epochs. Each time, the accuracy of the VGG-16 model was trained with a preprocessed dataset is higher than the VGG-16 model trained with a normal dataset. Thus, the preprocessed dataset optimizes the classification model's accuracy.

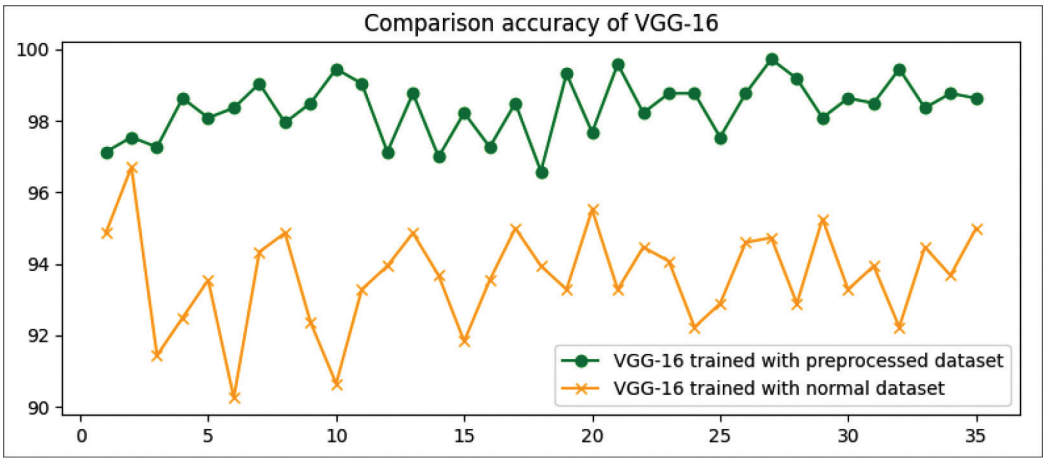

Fig. 9. The comparison accuracy between VGG-16 was trained with preprocessed dataset and VGG-16 was trained with normal dataset with 1000 epochs running in 35 times.

All of these models are compared to ones of our proposed model in order to verify that it is superior. The comparison of results between our proposed model and other comparative models by considering performance indicators are presented. Table II represents all indicators results obtained from different models based on the abnormities peeled shrimp classification running in 35 times. These models were trained with the preprocessed dataset by using the same parameter setting. The VGG-16 model provides higher accuracy than other competitive models with 98.36% and all indicators is accurate in the same high accuracy. It is clear that the VGG-16 is more accurate than other transfer learning models and supervised learning models.

The VGG-16 has a greater accuracy than a simple CNN because the fundamental architecture of the VGG-16 is based on CNN, but it is more complexity and has been trained with a larger dataset, so it will require less learning time and deliver a higher accuracy when trained with a new dataset.

Furthermore, The VGG-16 has a significantly greater accuracy as compared to SVM and RNN since it has a better feature extraction process by adding the convolutional layer and pooling layer connected in a complex architecture. This process will generate good attributes that are easy to classify in the classification layer. However, an RNN uses this process with only simple architecture and an SVM don't have these process.

Moreover, The VGG-16 is more accurate than other transfer learning methods. Every transfer learning approach is based on CNN with various degrees of complexity of architecture. The proper method should be well structured and have sufficient complexity in order to suit the new dataset. The outcome is the sole criterion for selecting a method. Therefore, the VGG-16 is suitable for this study.

The classification time and model size are important indicators for measuring the performance of the classification models. Since the classification model size directly affects the classification speed. The results show that the models that were built with complex architecture tend to be a larger size and often take a lot of time to classify than models that were built with minimal architecture. The VGG-16 was built 16 layers deep which is faster than the Resnet-50 which was built 50 layers deep. On the other hand, RNN is a less complicated architecture than the VGG-16, therefore it takes less classification time than the VGG-16. However, the complicatedness and size of classification models don't have an effect on classification accuracy.

In summary, even though all of the models are based on the abnormities peeled shrimps' classification. The VGG-16 with our designed classification layer was able to produce better results than the other competitive models and all indicators demonstrated the effectiveness of the VGG-16. Aligning and resizing images through data preprocessing is very important to increase the accuracy of our classification model. The size of models directly affects the classification times. The model with complex architecture tends to be large and it takes a long time to make a classification. The VGG-16 took less time to classify than the larger models. However, the model's size and classification speed do not affect the accuracy of classification models.

In order to evaluate the quality level of the results obtained from our proposed model. It is important to compare our proposed model with other competitive models since many models can investigate the abnormalities of peeled shrimp. CNN [29], RNN [30], and SVM [31] are commonly used classification approach, and there are frequently used as the preferred primary since many of the advanced models today are inspired by these models. MobileNet [32], Xception [33], Resnet-50 [34], Densnet [35], and Inception [36] are the transfer learning models that achieve the top class accuracy in ImageNet tests and are frequently used in classification tasks as the same things as the prior models.

IV. Conclusion

In this paper, a deep convolutional neural network with the VGG-16 based transfer learning for the abnormalities peeled shrimp classification is proposed. The major contribution of this work is the successful development of an effective methodology for classifying the abnormalities of peeled shrimp. The provided dataset was preprocessed by aligning images based on skeleton calculation, cropping images with the symmetrical bounding boxes, and resizing images to meet the need of the VGG-16 input layer requirement. The VGG-16 model was customized with our designed classification layers and was trained with our designed parameters. All indicator results obtained from our classification model show that the VGG-16 with our designed classification layer offers better accuracy than others. The preprocessed dataset with our method directly effects to increase the accuracy of classification models.

In future work, our provided method will be applied to the real production line. However, the peeled shrimps in the real production line are always stick together. The segmentation of stick peeled shrimp is our primary work.

Acknowlegment

We would like to thank the Digital Academy Thailand and the Faculty of Engineering at Sriracha, Kasetsart University, Sriracha Campus, for supporting the facilities for this study.

References

[1] M. Z. Herzberg, A. I. C. Córdova, and R. O. Cavallic, "Biological Viability of Producing White Shrimp Litopenaeus Vannamei in Seawater Floating Cages," *Aquaculture*, vol. 259, no. 1-4, pp. 283-289, Sep. 2006.

[2] A. Farhana, "The Export Trend of Shrimp Industries in Bangladesh: An Analysis," *Scientific Research Journal*, vol. 5, no. 4, pp. 80-95, Sep. 2017.

[3] R. Warangkhana, "Model for Forecasting the Export Volume of Frozen Shrimp," *RMUTSB Academic Journal*, vol. 8, no. 1, pp. 70-82, Jun. 2020.

[4] L. M. Díaz-Tenorio, F. García-Carreño, and Ramon Pacheco-Aguilar "Comparison of Freezing and Thawing Treatments On Muscle Properties of White Leg Shrimp (Litopenaeus Vannamei)," *Journal of Food Biochemistry*, vol. 31, no. 5, pp. 563-576, Oct. 2007.

[5] C. Jotikasthira, "The Development of Thailand's Potentials and Exports of Shrimp Processed for Southeast Asia," *Journal of Bangkokthonburi University*, vol. 8, no. 1, pp. 59-72, Jan. 2019.

[6] D. Sylvain, "Shrimp Quality and Safety Management Along the Supply Chain in Benin," Ph.D. thesis, Dept. Nutrition and Health Sciences, Wageningen Univ. Wageningen, NLD, 2015.

[7] G. A. Leiva-Valenzuela and J. M. Aguilera, "Automatic Detection of Orientation and Diseases in Blueberries Usingimage Analysis to Improve Their Postharvest Storage Quality," *Journal of Food Control*, vol. 33, pp. 166-173, Sep. 2013.

[8] H. Zareiforoush, S. Minaei, M. R. Alizadeh et al., "Design, Development And Performance Evaluation of an Automatic Control System for Rice Whitening Machine Based on Computer Vision and Fuzzy Logic," *Computers and Electronics in Agriculture*, vol. 124, pp. 14-22, Jun. 2016.

[9] P. A. Coelho, S. N. Torres, W. E. Ramírez et al., "A machine Vision System For Automatic Detection of Parasites Edotea Magellanicain Shell-off Cooked Clammulinia Edulis," *Journal of Food Engineering*, vol. 181, pp. 84-91, Jul. 2016.

[10] T. T. N. Thai, N. S. Thanh, and P. C. Viet, "Computer Vision Based Estimation of Shrimp Population Density and Size," in *Proc. International Symposium on Electrical and Electronoces (ISEE)*, 2021. pp.145-148.

[11] R. P. S. Sankar, V Jenitta, and B Kannapiran, "Diagnosis of Shrimp Condition Using Intelligent Technique," in *Proc. International Conference on Electrical, Instrumentation and Communication Engineering (ICEICE)*, 2017, pp.1-5.

[12] L. J. Dah, X. Guangming, R. M. Lane et al., "An Efficient Shape Analysis Method for Shrimp Quality Evaluation," in *Proc. International Conference on Control, Automation, Robotics and Vision (ICARCV)*, 2012, pp. 865-870.

[13] D. Zhang, K. D. Lillywhite, D. J. Lee et al., "Automatic Shrimp Shape Grading Using Evolution Constructed Features," *Computers and Electronics in Agriculture*, vol. 100, pp. 116-122, Jan. 2014.

[14] Z. Liu, C. Fang, and Z. Wei, "Recognition-Based Image Segmentation of Touching Pairs of Cooked Shrimp (Penaeus Orientalis) Using Improved Pruning Algorithm for Quality Measurement," *Journal of Food Engineering*, vol. 195, pp. 166-181, Feb. 2017.

[15] K. Weiss, T. M. Khoshgoftaar, and D. Wang, "A Survey of Transfer Learning," *Journal of Big Data*, pp. 1-40, May. 2016.

[16] K. Simonyan and A. Zisserman, "Very Deep Convolutional Networks for Large-Scale Image Recognition," *Computer Vision and Pattern Recognition*, vol. 6, pp. 1-14, Sep. 2015.

[17] G. Q. Jiang, C.-J. Zhao, and J.-Y. Qi, "The Research of Image Segmentation Based on Color Characteristic," in *Proc. International Conference on Machine Learning and Cybernetics*, 2011. pp 1-12,

[18] S. Bansal and D. Aggarwal, "Color Image Segmentation Using Cielab Color Space Using ant Colony Optimization," *International Journal of Computer Applications*, vol. 29, no. 9, pp. 28-34, Sep. 2011.

[19] P. Ganesan, V. Rajini, B. S. Sathish et al., "HSV Color Space Based Segmentation of Region of Interest in Satellite Images," in *Proc. International Conference on Control, Instrumentation, Communication and Computational Technologies*, 2014, pp. 1-10.

[20] C. Zhang, W. Yang, Z. Liu et al., "Color image segmentation in rgb color space based on color saliency," in *Proc. International Conference on Computer and Computing Technologies in Agriculture*, 2013, pp. 101-105.

[21] K. B. Shaik, P. Ganesan, and V. Kalist, "Comparative Study of Skin Color Detection And Segmentation in HSV and YCbCr

Color Space," *Procedia Computer Science*, vol. 57, pp. 41-48, Dec. 2015.
[22] N. Jamil, T. M. T. Sembok, and Z. A. Bakar, "Noise Removal and Enhancement of Binary Images Using Morphological Operations," in *Proc. International Symposium on Information Technology*, 2008, pp. 1-6.
[23] P. Maragos and R. W. Schafer, "Morphological Skeleton Representation and Coding of Binary Images," *IEEE Transactions on Acoustics, Speech, and Signal Processing*, vol. 34, no. 5, pp. 1228-1244, Oct. 1986.
[24] G. Toussaint, "Solving Geometric Problems with the Rotating Calipers," in *Proc. IEEE MELECON 83*, 2000, pp. 1-12.
[25] S. Suzuki and K. Abe, "Topological structural analysis of digitized binary images by border following," *Computer Vision, Graphics, and Image Processing*, vol. 30, no. 1, pp. 32-46, Apr. 1985.
[26] J. Gu, P. Yu, X. Lu et al., "Leaf Species Recognition Based on VGG16 Networks and Transfer Learning," in *Proc. IEEE 5th Advanced Information Technology, Electronic and Automation Control Conference*, 2021, pp. 2189-2193.
[27] M. Sokolova, N. Japkowicz, and S. Szpakowicz, "Beyond Accuracy, F-Score and Roc: A Family of Discriminant Measures For Performance Evaluation," *Advances in Artificial Intelligence*, vol. 4304, pp. 1015-1021, Jan. 2006.
[28] T. Viering and M. Loog, "The Shape of Learning Curves: A Review," *ArXiv*, vol. 1, pp. 1-46, Mar. 2021.
[29] A. Saad, A. M. Tareq, and A.-Z. Saad, "Understanding of a Convolutional Neural Network," in *Proc. International Conference on Engineering and Technology*, 2017, pp. 1-6.
[30] B. Siddhartha, S. Václav, and K. Ashish. *Recurrent Neural Network*. Elsevier Academic Press, Massachusetts: USA, 2020, pp. 52-64.
[31] Z. Yongli, "Support Vector Machine Classification Algorithm and its Application," in *Proc. International Conference on Information Computing and Applications*, 2012, pp.179-186.
[32] A. G. Howard, M. Zhu, B. Chen et al., "Mobilenets: Efficient Convolutional Neural Networks for Mobile Vision Applications," *Computer Vision and Pattern Recognition*, vol. 1, pp. 1-9, Apr. 2017.
[33] F. Chollet, "Xception: Deep Learning with Depthwise Separable Convolutions," in *Proc. IEEE Conference on Computer Vision and Pattern Recognition*, 2017, pp. 1-8.
[34] K. He, X. Zhang, S. Ren et al., "Deep residual Learning for Image Recognition," in *Proc. IEEE Conference on Computer Vision and Pattern Recognition*, 2016 pp. 770-778.
[35] G. Huang, Z. Liu, L. V. D. Maaten et al., "Densely Connected Convolutional Networks," in *Proc. IEEE Conference on Computer Vision and Pattern Recognition*, 2018, pp. 1-9.
[36] C. Szegedy, V. Vanhoucke, S. Ioffe et al., "Rethinking the Inception Architecture for Computer Vision," in *Proc. IEEE Conference Computer Vision and Pattern Recognition*, 2015, pp. 4700-4708.

Tamnuwat Valeeprakhon is a lecturer at the Department of Computer Engineering, Faculty of Engineering at Sriracha, Kasetsart University, Sriracha campus, Thailand. He graduated M.Eng in Computer Engineering from Khon Kaen University, Thailand. He was granted a scholarship from the National Science and Technology Development Agency (NSTDA) for studying at the Kochi University of Technology, Japan. His research interests including of Computer Vision, Image Processing, and Artificial Intelligence.

Korawit Orkphol is a lecturer at the Department of Computer Engineering, Faculty of Engineering at Sriracha, Kasetsart University, Sriracha campus, Thailand. He graduated Ph.D. in Computer Science and Technology from Harbin Engineering University, P.R. Harbin, China. His research field including of Artificial Intelligence, Machine Learning, and Natural Language Processing.

Penpun Chaihuadjaroen is an Assistant Professor at the Department of Computer Engineering, Faculty of Engineering at Sriracha, Kasetsart University, Sriracha campus, Thailand. She graduated M.S in Computer Science from King Mongkut's Institute of Technology Ladkrabang, Thailand. Her research field including of Computer Vision and Image Processing.